

Cell Reports, Volume 28

Supplemental Information

**Complex Economic Behavior Patterns
Are Constructed from Finite, Genetically
Controlled Modules of Behavior**

Cornelia N. Stacher Hörndli, Eleanor Wong, Elliott Ferris, Kathleen Bennett, Susan Steinwand, Alexis Nikole Rhodes, P. Thomas Fletcher, and Christopher Gregg

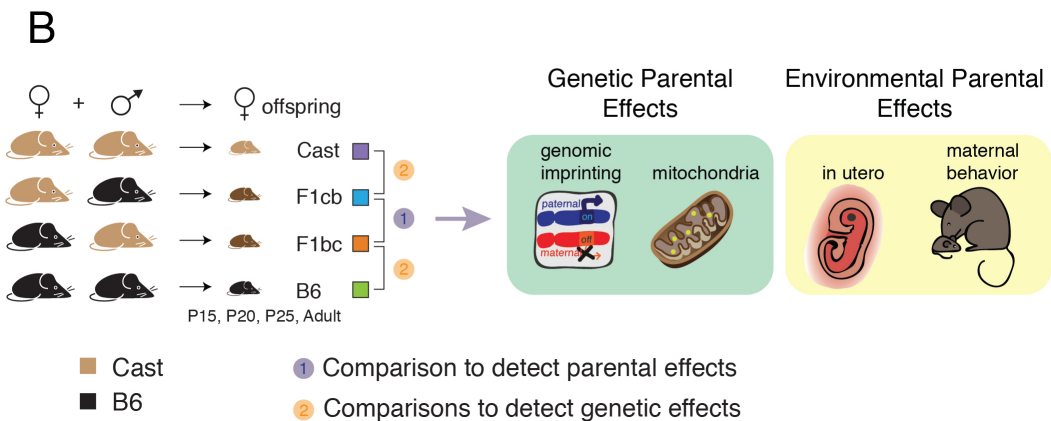
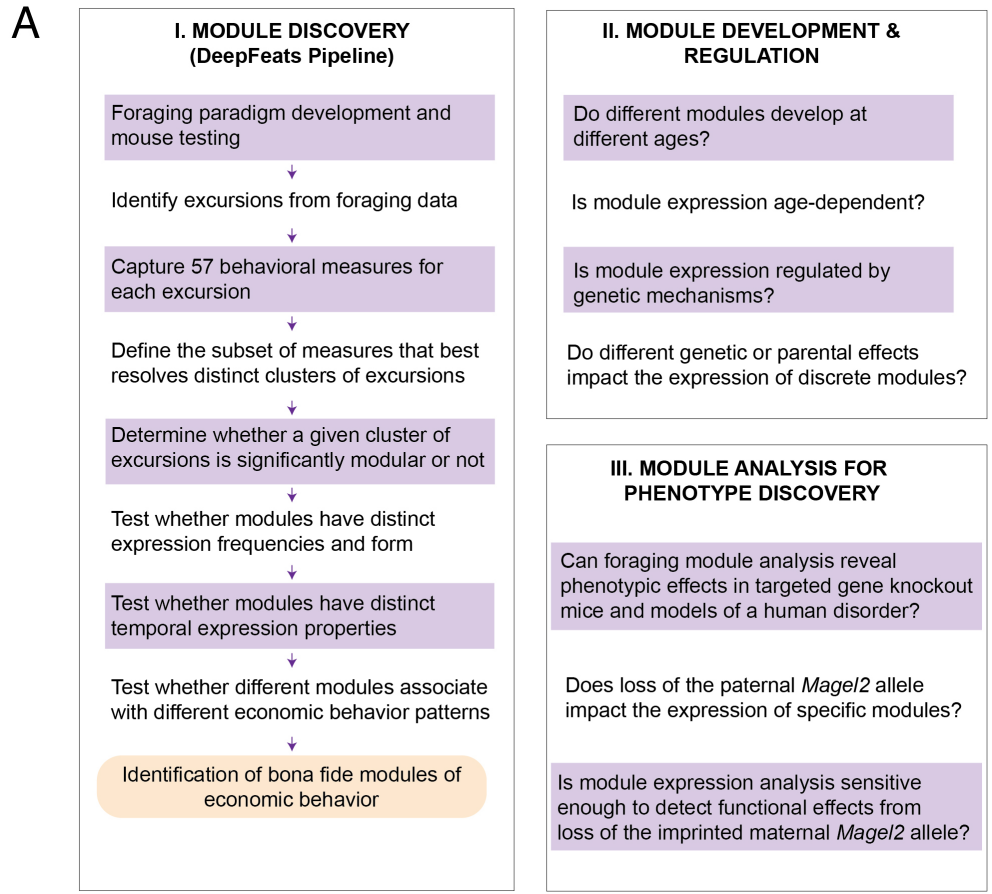


Figure S1. An overview of the study and mouse genetics strategy to test for developmental, genetic and parental effects on foraging module expression. Related to Figure 1.

(A) The schematic depicts the logical flow and structure of our manuscript. (I) Shows an overview of the DeepFeats workflow to identify modules of behavior from complex foraging patterns. (II) Our study applies this knowledge and methodology to test

whether modules are discrete units of behavior regulated by developmental, genetic and parental effects in mice. (III) Finally, by analyzing *Mage12* mutant mice, a model of PWS, we test whether specific mechanisms can be mapped onto specific modules and whether module profiling is a sensitive and robust platform for phenotype analysis.

(B) Schematic summary of mouse genetics strategy to identify parental and/or genetic effects at P15, P20, P25 and adulthood. Different mice are tested at each age, so the animals are naïve to the test. Parental effects in this design potentially encompass genetic parental effects and environmental parental effects (see text).

A Resampling Test of Excursion Clusters Based on Retained Measures

- 10000x
1. Randomly sample behavioral measures with replacement
 2. Cluster the data (Ward) and define clusters with dynamic tree cut
 3. Count total number of clusters found
 4. Compare observed to resampled distribution and compute p-value

B Results of Resampling Test (Behavioral Measures filtered at $r < 0.4$)

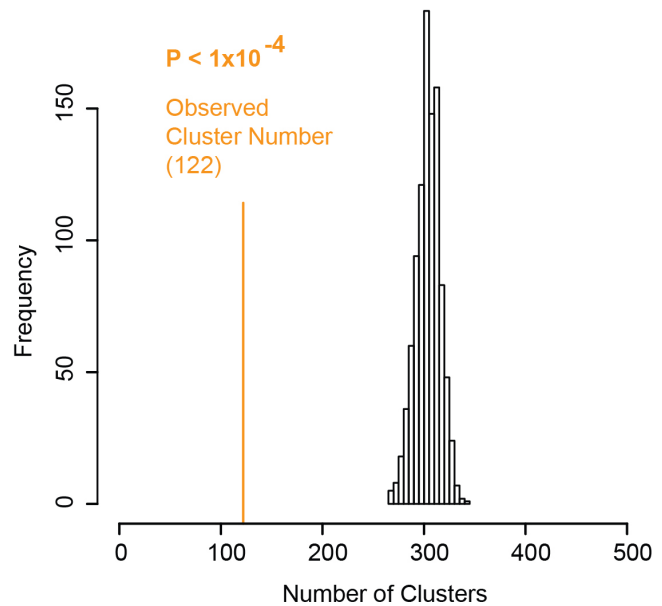


Figure S2. Resampling test determined that the 13 retained behavioral measures resolve significant clusters of excursions. Related to Figure 2.

(A and B) A sampling test is performed to test whether the $r < +0.4$ behavioral measures yield significant clustering compared to randomly sampled $r < 0.4$ behavioral measure data, which breaks relationships between excursions and measures. The resampling testing approach is shown in (A). The results indicate significant clustering effects with the $r < 0.4$ retained behavioral measures ($P < 1 \times 10^{-4}$; lower tail test) (B). Black bars show the number of clusters detected from randomly sampled behavioral measures and the orange line indicates the observed number.

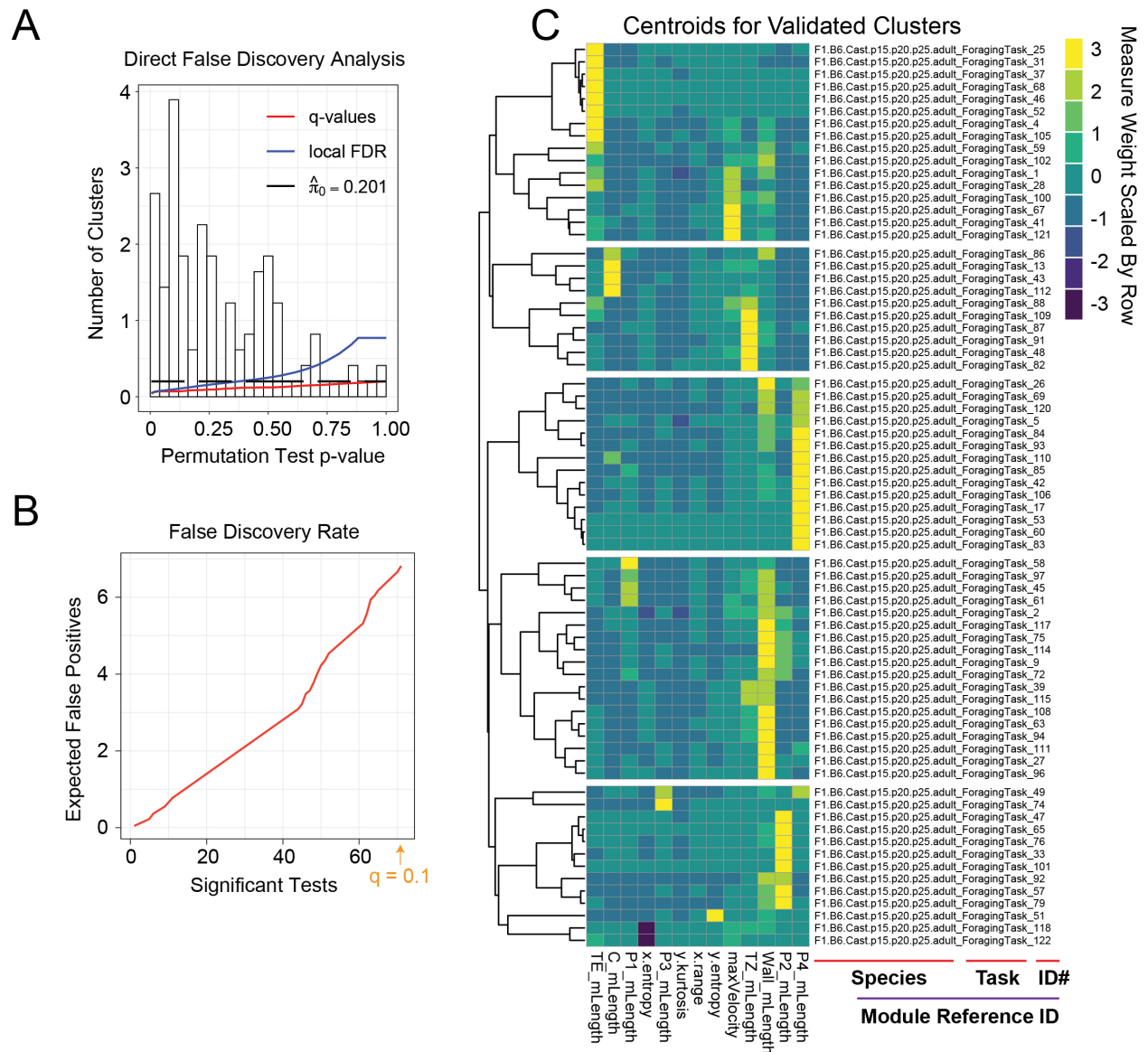


Figure S3. Significant modules of foraging behavior have unique characteristics that are revealed from the module centroids. Related to Figure 3.

(A and B) The plots show the results of the direct estimate of false positives using a q-value analysis of the IGP permutation test p-values computed for the 122 clusters in the training data partition. The histogram of the number of clusters with different p-values indicates a left shifted distribution consistent with many significant effects (ie. reproducible clusters) (A). The local false discovery rate (blue) is shown, as well as the estimated proportion of true null p-values (black dashed line) and the p-value cutoff

when the q-value captures all true positives (red line, q-value). (B) The estimated false discoveries for different numbers of tests indicates 6 to 7 false positives among the 71 clusters defined as significant at $q < 0.1$. This q-value cutoff balances type I errors for the identification of modules and type II errors for the identification of nonmodular excursion types. The q-value results also show that 20% of the 122 total clusters (24) are true nulls and therefore true nonmodular ($\pi_0 = 0.201$).

(C) The heatmap shows the centroids for each significant module of behavior. The centroids are the mean values of the behavioral measures calculated from the excursions assigned to a given module. The identity of the behavioral measures is shown on the X axis. The data has been clustered to group centroids with related patterns, though each centroid weights the behavioral measures differently. The data is scaled by row to show the relative weights. The centroids for each module are stored for reference by an ID that records the mouse strain, ages and behavioral task in which they were found, as well as a unique number. The module number is the number of the original cluster found to be reproducible by IGP analysis. TE, tunnel entry zone; C, arena center zone; P1-4, Pots 1-4; X, movement in the X dimension; Y, movement in the Y dimension; TZ, tunnel zone; Wall, arena wall zone; mLength, mean length of time (seconds); range, range of distance traveled; entropy, entropy of movement; kurtosis, kurtosis of the distribution of movement in the Y dimension; maxVelocity, maximum velocity detected during the excursion.

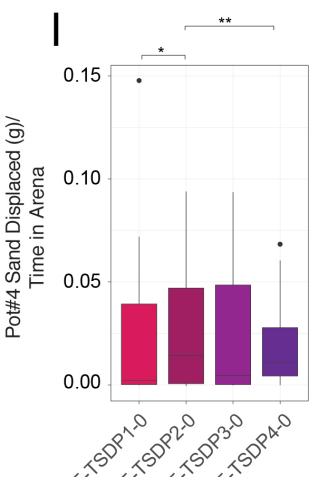
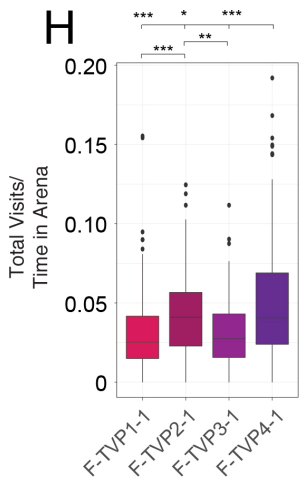
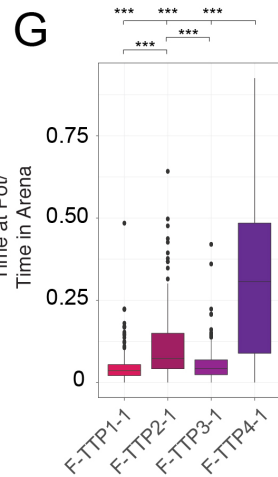
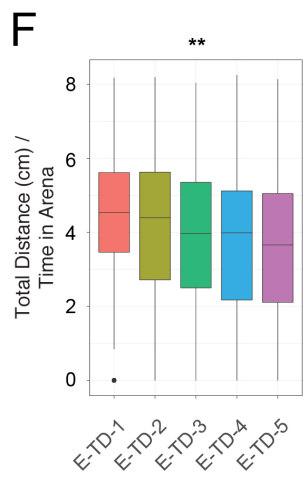
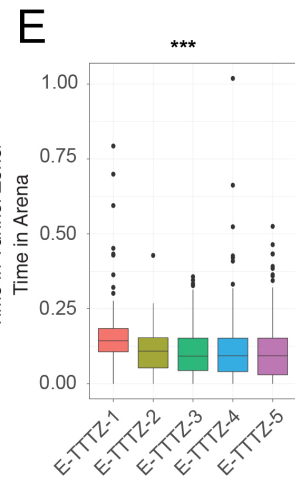
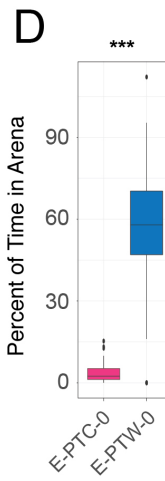
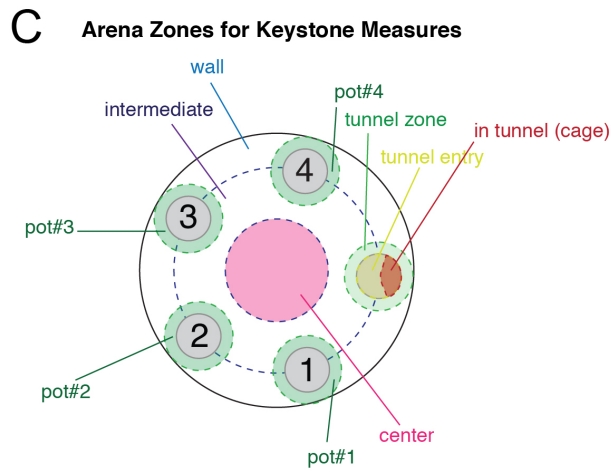
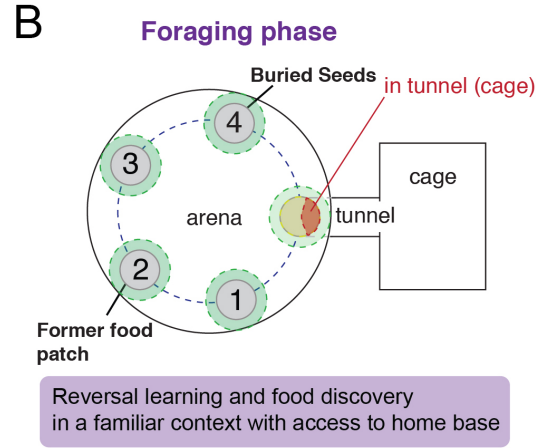
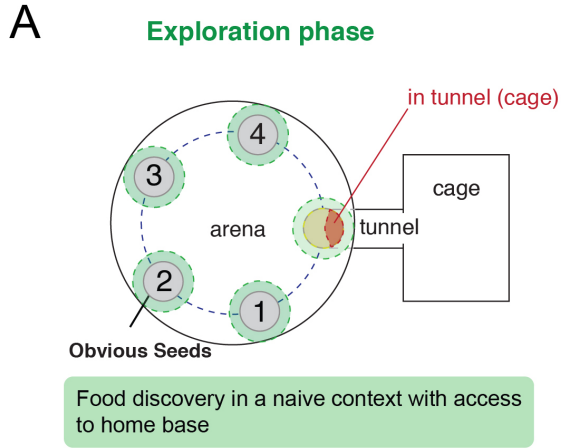


Figure S4. Identification of keystone foraging measures describing diverse feeding, exposure, activity and memory/perseveration response patterns. Related to Figure 5.

(A and B) Schematic overviews of the arena layout during the Exploration (A) and Foraging (B) phases of the assay.

(C) Deconstruction of the arena into the wall zone (wall) and center zone (center), pot zones and tunnel zone to measure time and visits to important elements of the arena for analyses of feeding, exposure, activity and perservation patterns.

(D and E) Box plots show measures of exposure during foraging. (D) The percentage of time spent in the center (PTC) versus wall (PTW) zones in the Exploration (E-) phase over the whole trial (-0) is shown for all F1cb, F1bc and B6 animals tested. Significantly more time is spent in the wall zone ($P < 2 \times 10^{-16}$, Welch's two sample t-test, $df=182.9$).

(E) Shows the total time spent in the tunnel zone (TTTZ) in the Exploration phase (E-) in 5 minute time bins (-1, -2, -3, -4, -5). A significant main effect of time bin is observed ($P < 2 \times 10^{-6}$, one way ANOVA, $F=8.0$ on 4 and 875 degrees of freedom), with more time in the tunnel zone in the first 5 minutes of the assay (-1). The data show mice prefer sheltered over exposed regions, as expected.

(F) Box plots show measures of activity from the total distance (TD) traveled during foraging. Data is shown for 5-minute time bins. A significant main effect of time bin on distance traveled is observed ($P = 0.002$, one way ANOVA, $F=4.3$ on 4 and 875 degrees of freedom) and the data indicate relatively greater distances are traveled during earlier time bins.

(G-I) Box plots show measures of memory & perseveration responses in the Foraging phase. (G) A significant increase in the total time at the former food pot, Pot 2 (TTP2), is observed in the Foraging phase (F-) in the first 5 minutes of the trial compared to pots without food associations (Pot1 (P1) and Pot2 (P2)) ($P < 2 \times 10^{-16}$, ANOVA and Tukey HSD post-test results shown, $F=148.4$ on 3 and 700 degrees of freedom), showing the effect of the memory. Total time at the new food pot (Pot4 (P4)) is also significantly increased. (H) Shows the total number of visits to the different pots (TVP) during first 5 minute time bin of the Foraging phase. A relative increase in the number of visits to the former (P2) and new food pots (P4) is observed compared to those not food associated

(P1 and P3) ($P < 2 \times 10^{-16}$, ANOVA and Tukey HSD post-test results shown, $F=20.4$ on 3 and 700 degrees of freedom), which also shows perseveration effects of the memory. (I) The plots shows the total sand dug from each pot (TSDP) over the whole Foraging phase (F-) trial (-0). A significant main effect of pot was found and involves relatively increased digging in the former food pot (P2) and new food pot (P4) ($P = 0.003$, one way ANOVA and Tukey HSD post-test results shown, $F=4.6$ on 3 and 700 degrees of freedom). Thus, different measures capture different perseveration response patterns. Tukey posttest p-adjust: *** < 0.001 , ** <0.01 , * <0.05 . $N=179$ mice.

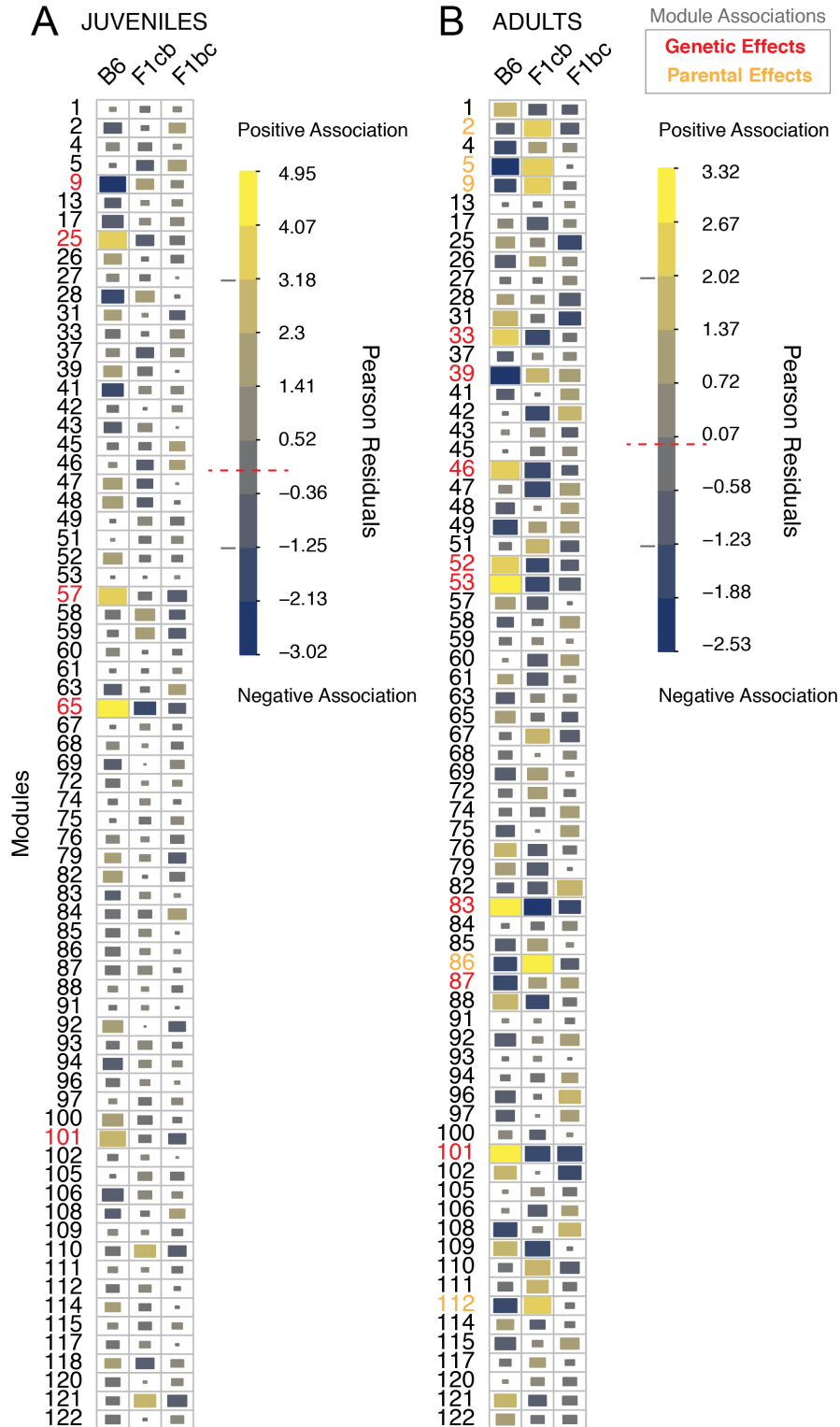


Figure S5. Genetic and parental effects regulate module expression and map onto specific modules at different ages. Related to Figure 6.

(A-B) The charts show the top modules impacted by genetic (red modules) and parental (orange modules) effects in juveniles (A) and adults (B). The Pearson residuals from a Chi-Square test of independence between modules and different genotypes and parental crosses are shown and based on module expression frequency data. The data show modules with expression frequencies that are positively (yellow) and negatively (blue) associated with each mouse strain. Relative association effect size is depicted by color (see legend) and block size. Specific modules are strongly impacted by genetic differences between B6 and F1bc (red), or parental differences between F1cb and F1bc (orange). The red dashed line in the legend shows the threshold at which the observed and expected module expression counts are the same (Pearson residuals equal zero). The grey lines show the threshold for the top affected modules. Juveniles: B6 N= 31, F1cb N=45, F1bc N=48; Adults: B6 N= 20, F1cb N=17, F1bc N=18.

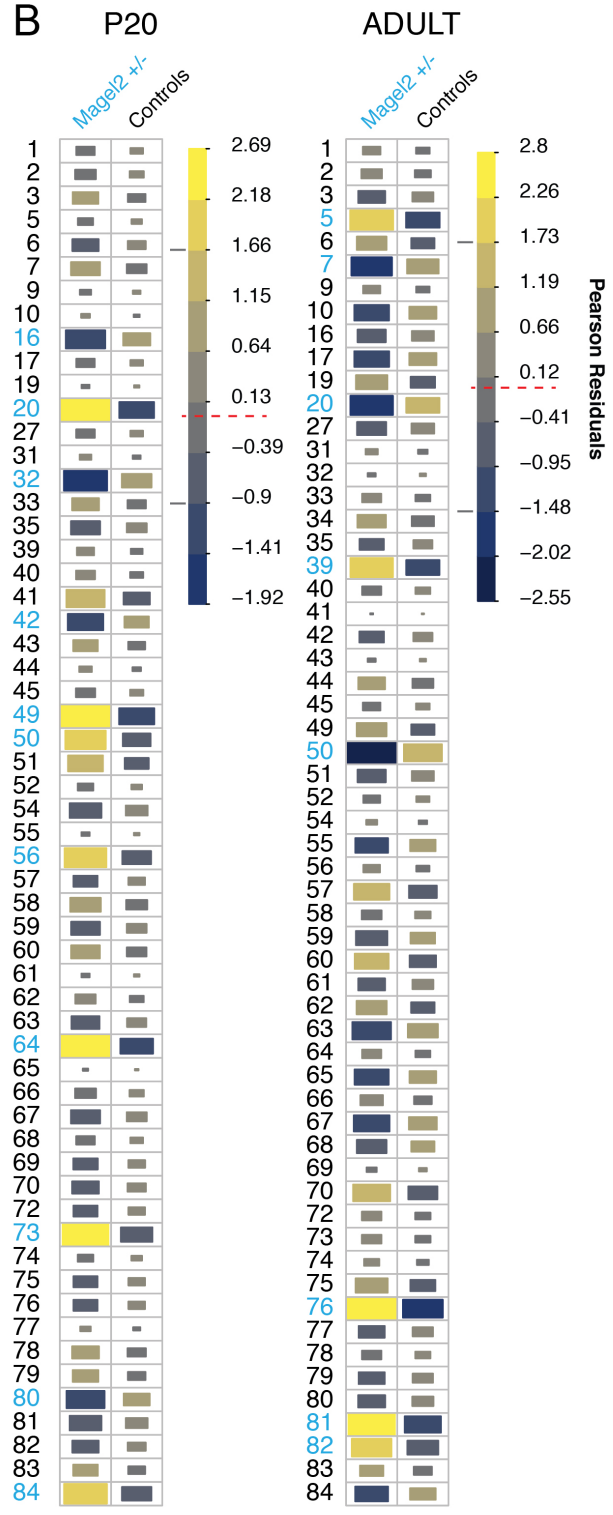
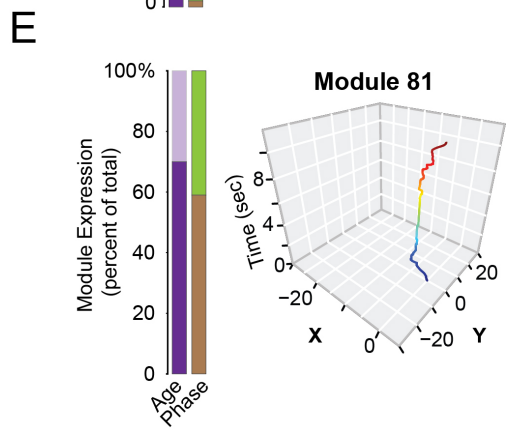
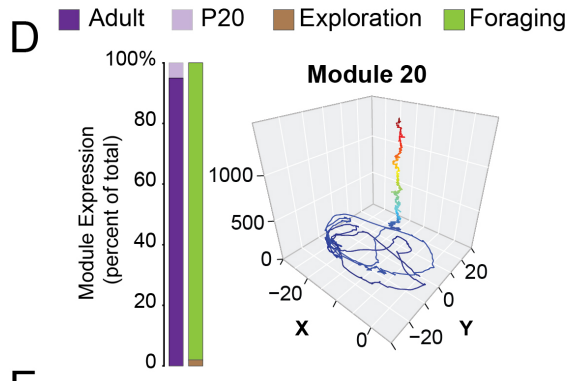
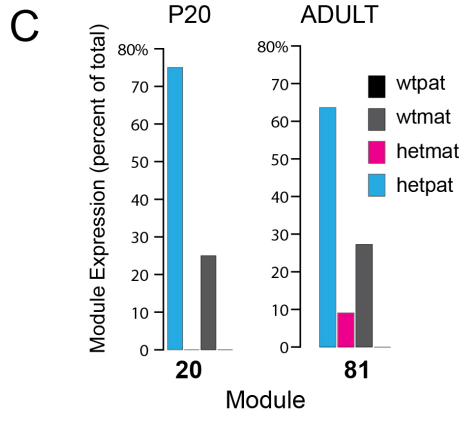
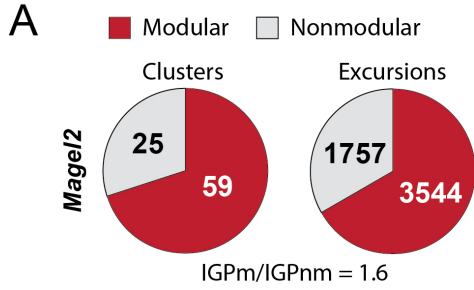


Figure S6. Loss of the paternal *MageI2* allele causes significant changes to the expression of a defined subset of modules in juveniles and adults. Related to Figure 7.

(A) Pie charts show the number of modules ($q < 0.1$) and nonmodular ($q > 0.1$) clusters and excursions identified from foraging excursions performed by adult and P20 *MageI2*^{+/-} mutants and controls (*MageI2*^{-/+}, ^{+/+}) (IGP permutation test, see Fig. 8-S1).

(B) The charts show the modules affected by loss of the paternal *MageI2* allele in P20 juveniles and adults (highlighted in blue). The charts plot the Pearson residuals computed from a Chi-Square test of independence between modules and *MageI2*^{+/-} mutants versus controls (*MageI2*^{+/+}, *MageI2*^{-/+}) for P20 juveniles and adults. The data show modules with expression frequencies that are positively (yellow) and negatively (blue) associated with *MageI2*^{+/-} mutants versus controls. Relative effect size is depicted by color (see legend) and block size and the most affected modules are highlighted (blue numbers). The data show specific modules are impacted by loss of the paternal *MageI2* allele. The red dashed line in the legend shows the threshold at which the observed and expected module expression counts are the same (Pearson residuals equal zero). The grey lines show the threshold for the top affected modules. For *MageI2* at P20/Adult: N=22/18 maternal wt (*MageI2*^{m+/p+}), N=28/23 maternal het (*MageI2*^{m-/p+}), N=22/20 paternal wt (*MageI2*^{m+/p+}) and N=22/20 paternal het (*MageI2*^{m+/p-}).

(C) The bar plots show the percentage of excursions that are expressed by the different *MageI2* genotypes for module 20 in P20 juveniles and module 81 in adults (relates to B). Both modules show preferential expression by *MageI2*^{+/-} mutants (hetpat) compared to controls (*MageI2*^{+/+}, wtpat; *MageI2*^{+/+}, wtmat; *MageI2*^{-/+}, hetmat).

(D-E) The stacked barplots show the proportion of excursions expressed by each age and in each phase for modules 20 and 81. The X-Y movement traces show representative excursions for each module. Modules 20 and 81 have expression effects that distinguish *MageI2*^{+/-} mutants from controls (see B,C). (D) Module 20 involves surveys of the arena and a very long (>1000 sec) stay at the food pot (Pot#4) in the Foraging phase that runs to the end of the 25 minute trial. This module is almost exclusively expressed by adults with the exception of P20 *MageI2*^{+/-} mutants (see C). (E) Module 81 involves lingering near the entry to the tunnel zone for several seconds

and is expressed by adults (purple bar) and P20 juveniles (blue bar) in the Exploration (brown) and Foraging (green) phases.

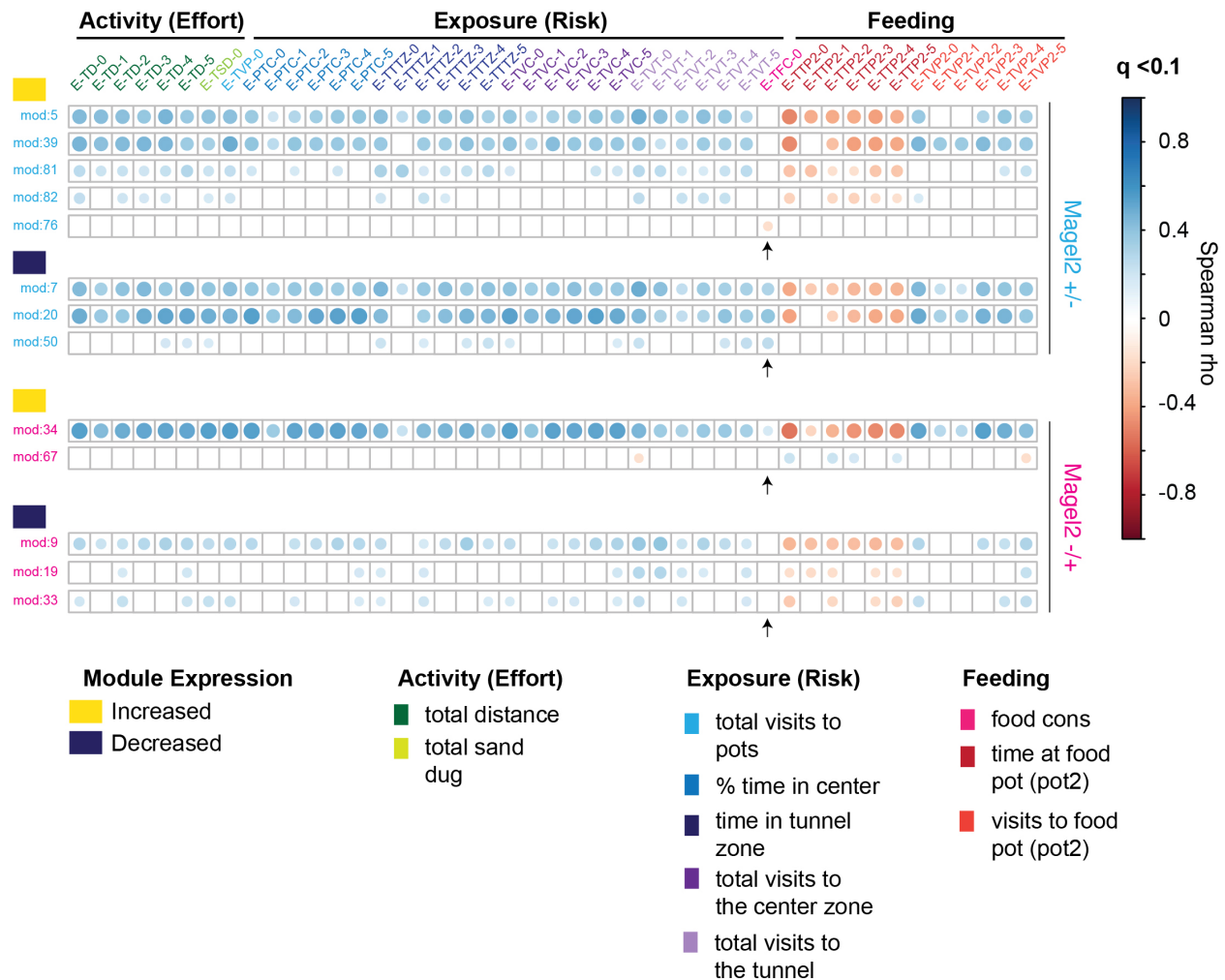


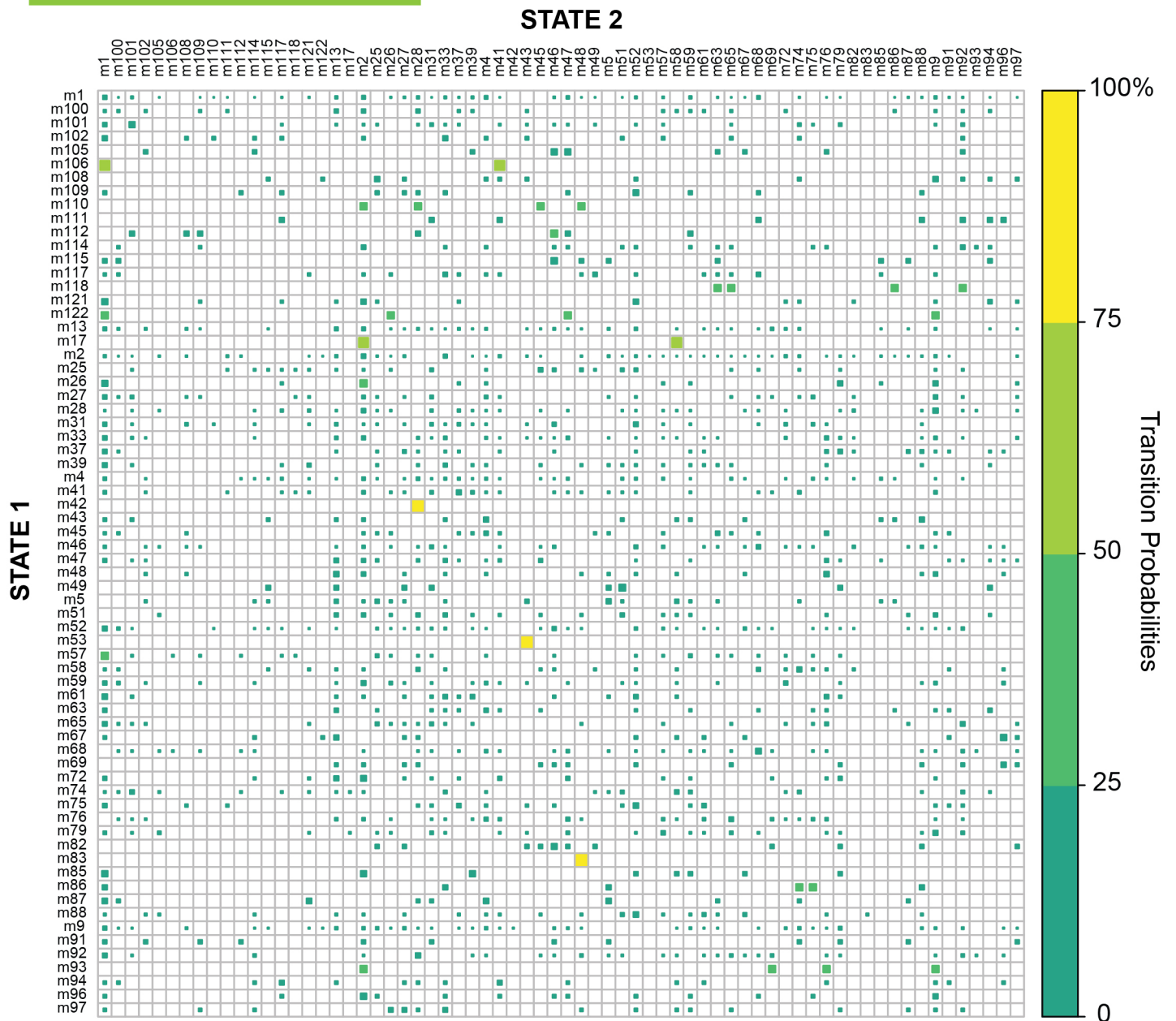
Figure S7. Loss of the maternal versus paternal *Mage12* alleles affects different modules that are linked to different economic behavior patterns. Related to Figure 7.

The plot shows the relationship between the top modules affected by loss of the paternal (blue) versus maternal (pink) *Mage12* alleles and specific keystone measures of foraging. The plot shows statistically significant correlations between the indicated modules (mod, rows) and keystone measures of foraging activity, exposure and feeding patterns in the Exploration phase. The correlations are calculated using the Spearman test for data collected for all *Mage12* genotypes and ages and p-values are corrected for multiple testing using the q-value method across both Exploration and Foraging phase tests ($q < 0.1$). White squares indicate no significant correlation detected ($q > 0.1$). The

magnitude of significant positive (blue) and negative (red) correlations between modules and keystone features are indicated by dot size and shade (see legend). Data is shown for modules with increased (yellow block) or decreased (dark blue block) expression in adult *Mage12*^{+/-} (blue) (see Figure S6B) or *Mage12*^{-/+} mice (pink) (see Figure 7E). The data show that the different modules increased and decreased by the different parental alleles are associated with different economic behavior patterns (see main text). The black arrow indicates module links to total food consumed (E-TFC-0). For further definitions of keystone features see Table S2.

SUPPLEMENTAL DATA

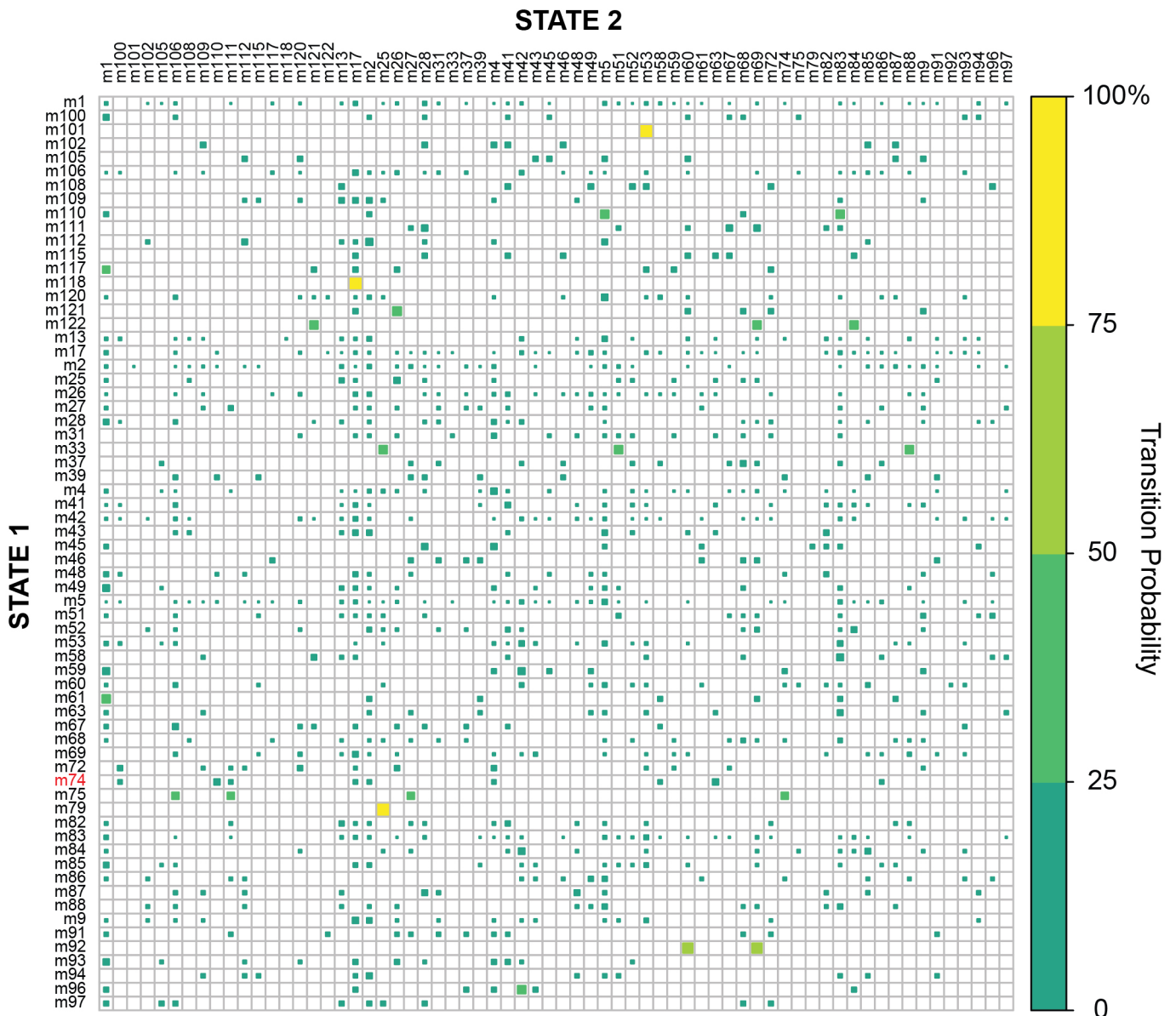
EXPLORATION PHASE (**P = 0.009)



Data S1. Probabilistically determined module expression orders in the Exploration phase. Relates to Figure 4.

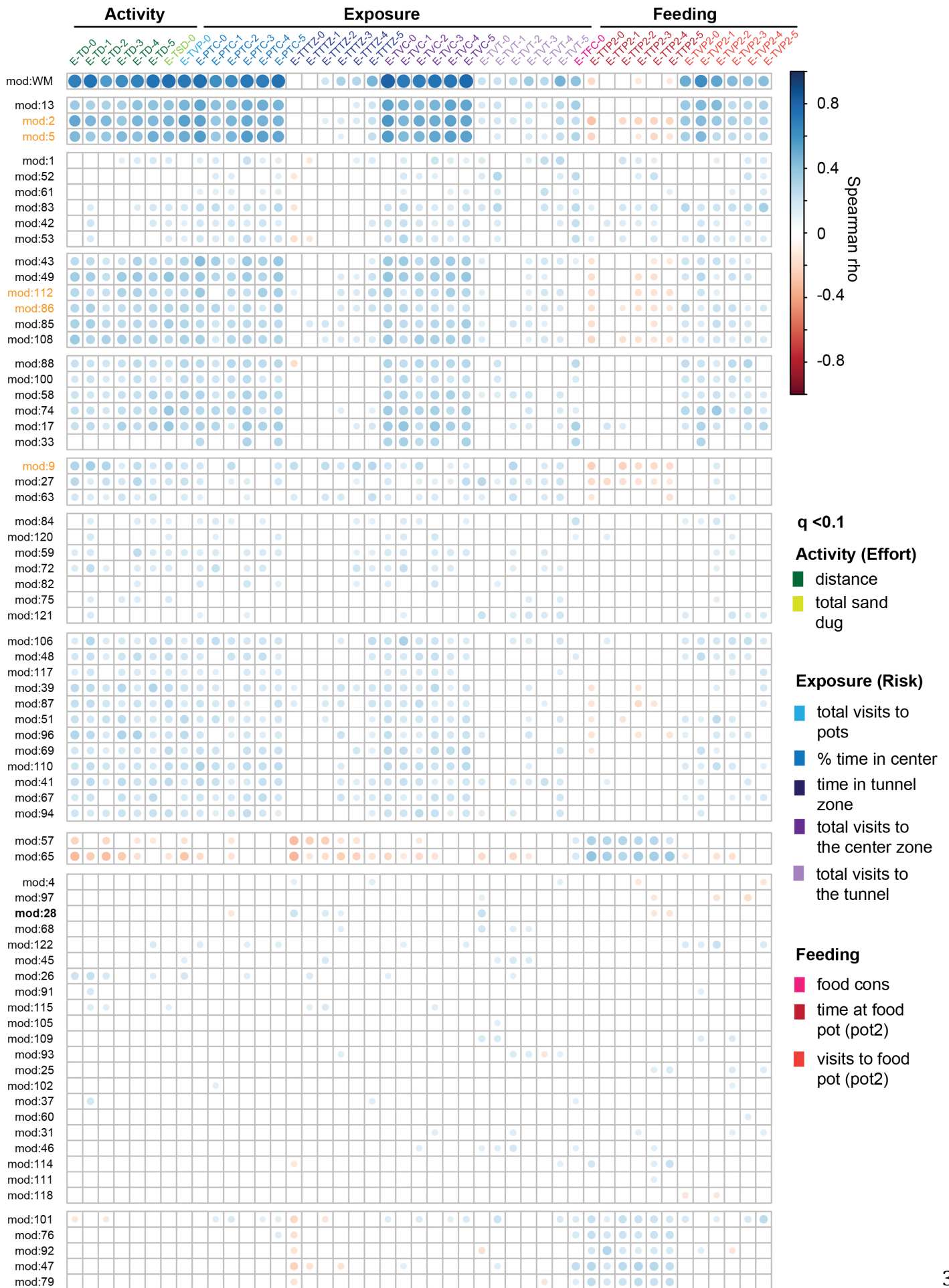
The chart shows the transition probabilities between modules in the naïve Exploration phase. The starting state modules are presented on the y-axis (State 1) and the transition state modules are on the x-axis (State 2). The plot is computed from a transition matrix of the number of times each transition type occurred. The data show that transitions between modules depend significantly on the type of module initially expressed (state 1) (Fisher’s Exact Test, $P=0.009$, two sided test, Monte Carlo simulated p-value). The strength of the transition probability is indicated by the size and shade of the box as shown in the legend. If a box is not shown, no association exists.

FORAGING PHASE (P = 0.00001)**



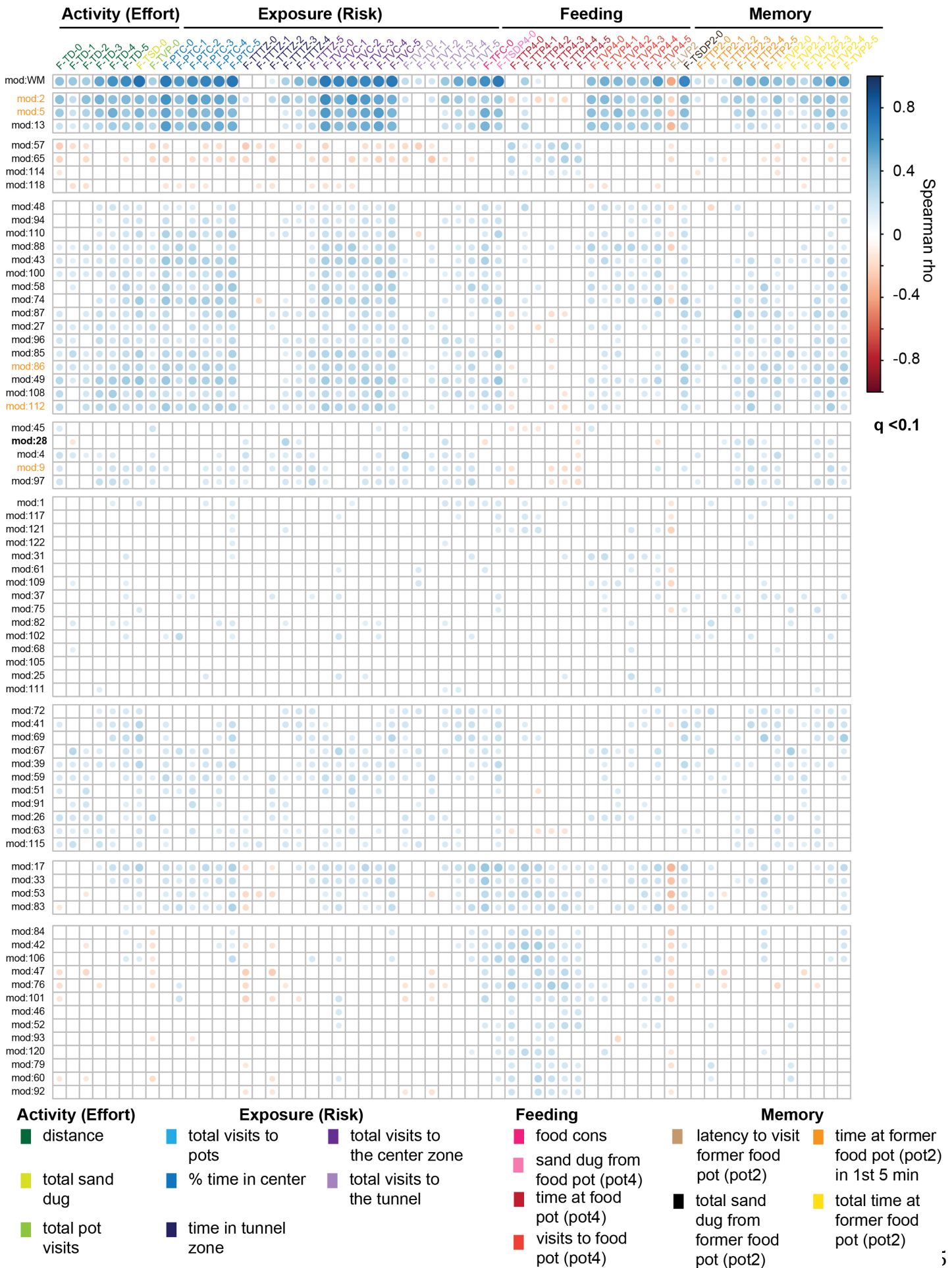
Data S2. Probabilistically determined module expression orders in the Foraging phase. Relates to Figure 4.

The chart shows the transition probabilities between modules in the familiar Foraging phase. The starting state modules are presented on the y-axis (State 1) and the transition state modules are on the x-axis (State 2). The plot is computed from a transition matrix of the number of times each transition type occurred. The data show that transitions between modules depend significantly on the type of module initially expressed (state 1) (Fisher’s Exact Test, $P=1 \times 10^{-5}$, two sided test, Monte Carlo simulated p-value). The strength of the transition probability is indicated by the size and shade of the box as shown in the legend. If a box is not shown, no association exists. Module 74 (red) is a highlighted example in the main text and Fig. 4E.



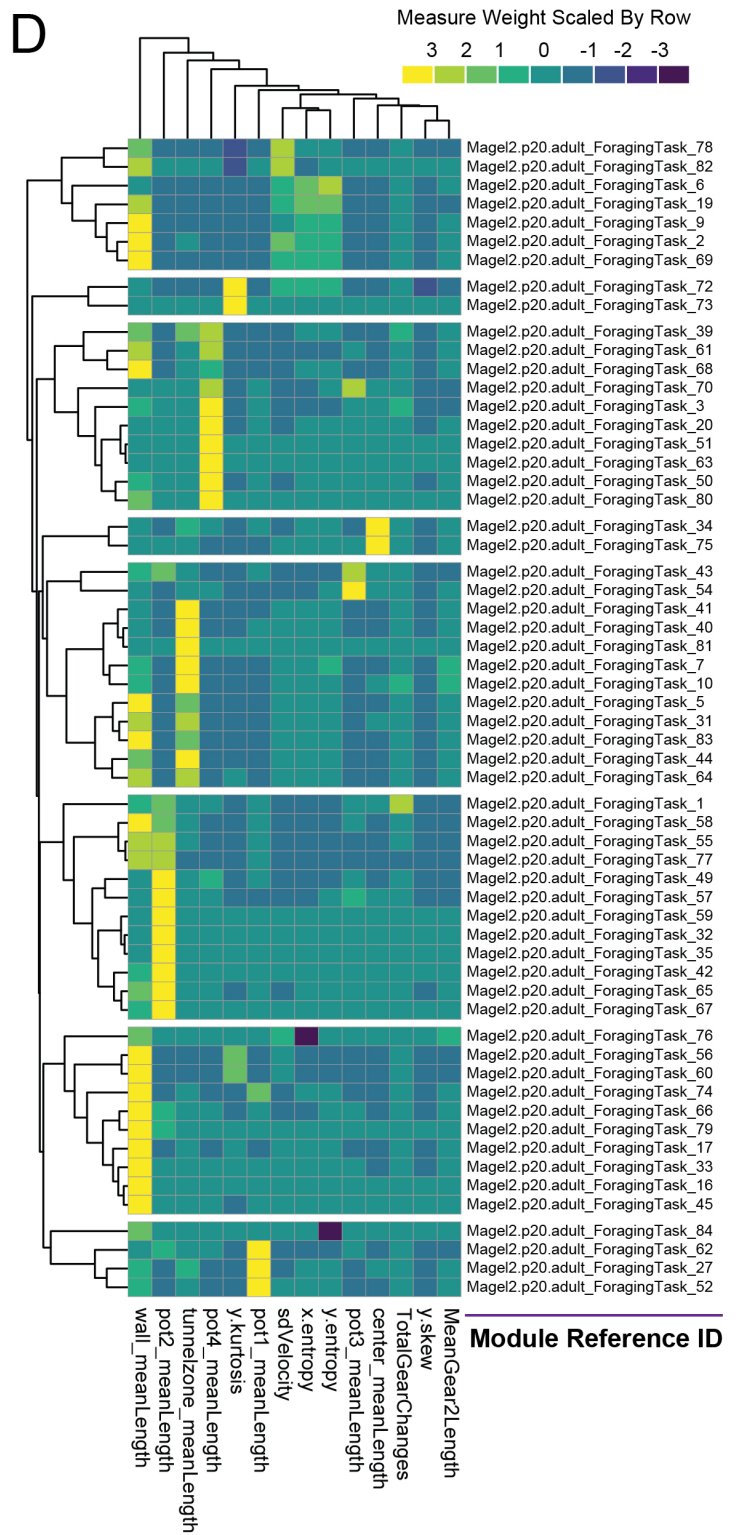
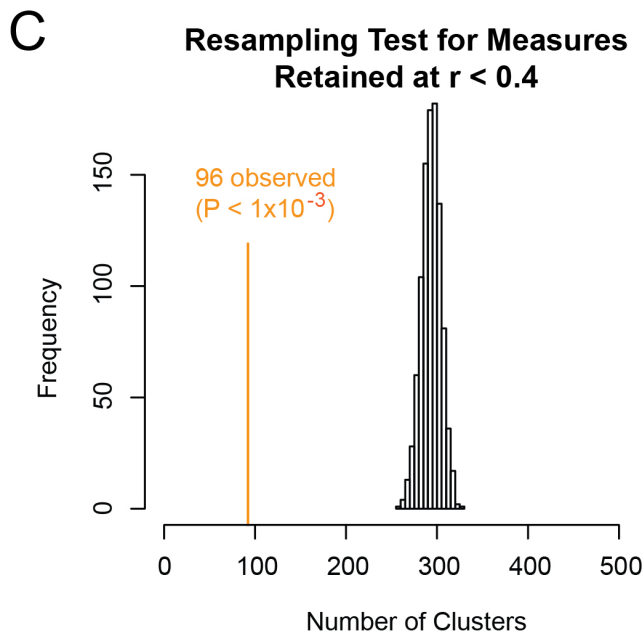
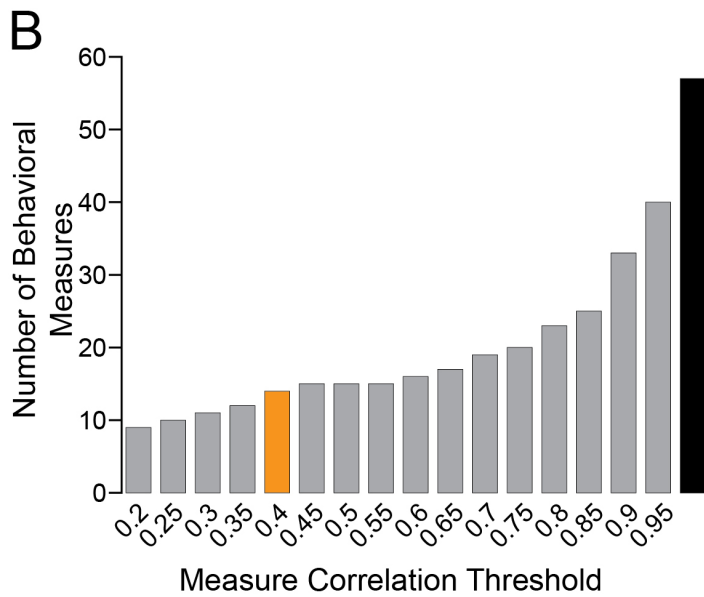
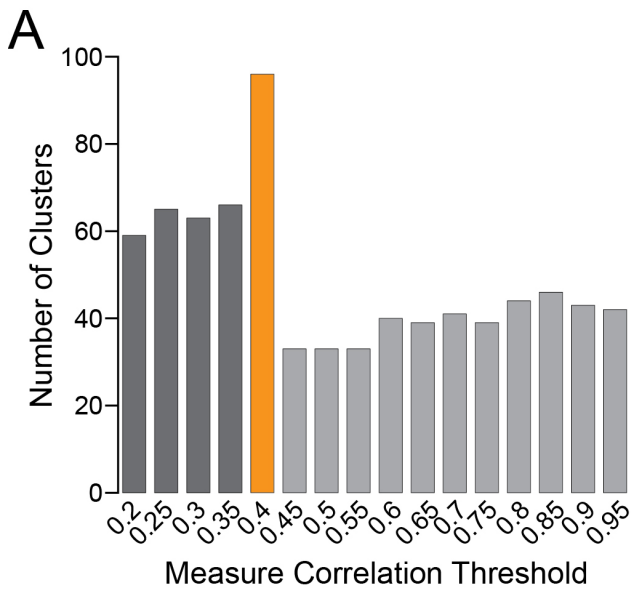
Data S3. Correlations between individual modules and keystone measures reveal different modules link to different economic behavior patterns in the Exploration phase. Relates to Figure 5.

The correlation plot shows statistically significant correlations between the indicated modules (mod, rows) and keystone measures of foraging activity, exposure and feeding patterns in the Exploration phase (E-). The correlations are calculated using the Spearman test for data collected for all strains and ages and p-values are corrected for multiple testing using the q-value method across both Exploration and Foraging phase tests ($q < 0.1$). White squares indicate no significant correlation detected ($q > 0.1$). The magnitude of significant positive (blue) and negative (red) correlations between modules and keystone features are indicated by dot size and shade (see legend). For further definitions of keystone features see Table S3. The different 5-minute time bins for some measures are indicated by numbers (-1, -2, -3, -4, -5) over the 25-minute trial. Data aggregated over the whole trial is indicated by "-0". The bold (developmental effect) and orange (parental effect) highlighted modules are examples detailed in the main text.



Data S4. Correlations between individual modules and keystone measures reveal different modules link to different economic behavior patterns in the Foraging phase. Relates to Figure 5.

The correlation plot shows statistically significant correlations between the indicated modules (mod, rows) and keystone measures of foraging activity, exposure, feeding and memory & perseveration patterns in the Foraging phase (F-). The correlations are calculated using the Spearman test for data collected for all strains and ages and p-values are corrected for multiple testing using the q-value method across both Exploration and Foraging phase tests ($q < 0.1$). White squares indicate no significant correlation detected ($q > 0.1$). The magnitude of significant positive (blue) and negative (red) correlations between modules and keystone features are indicated by dot size and shade (see legend). For further definitions of keystone features see Table S3. The different 5-minute time bins for some measures are indicated by numbers (-1, -2, -3, -4, -5) over the 25-minute trial. Data aggregated over the whole trial is indicated by “-0”. The bold (developmental effect) and orange (parental effect) highlighted modules are examples detailed in the main text.



Data S5. Identification of modules and nonmodular excursions from adult and P20 *Mage12* Mutant and Control Mice using the DeepFeats Approach. Relates to Figure 7.

(A) The bar plot shows the number of clusters obtained from behavioral measures pruned at different Pearson correlation thresholds from $r < 0.2$ -to- 0.95 . The data show that $r < 0.4$ yields the finest resolution of clusters in the *Mage12* data, identifying a total of 96 clusters (orange bar).

(B) The bar plot shows the number of behavioral measures retained at different correlation thresholds. The total number measured is 57 (black bar). The number of measures retained at the $r < 0.4$ threshold is 14 (orange bar).

(C) The results of a resampling test for significant clustering effects based on the *Mage12* $r < 0.4$ behavioral measure data are shown. The distribution of the number of clusters detected for each random sampling iteration is shown (10000 iterations). The observed number of clusters is significantly less than the null distribution indicating significant clustering (lower tail test).

(D) The heatmap shows the centroids for each significant module of behavior for the *Mage12* mice. The centroids are the mean values of each retained measure computed across all of the excursions assigned to a significant cluster ($q < 0.1$, IGP permutation test). The identity of the measures defined at the $r < 0.4$ threshold are shown on the x-axis. Each measure is scaled by row to show the relative weights. The data has been clustered to indicate centroids with related patterns, though each weights the 14 different measures differently. The module centroids are stored for reference by an ID that records the mouse strain, ages and behavioral task in which they were found, as well as a unique number. TE, tunnel entry zone; C, arena center zone; P1-4, Pots 1-4; X, movement in the X dimension; Y, movement in the Y dimension; TZ, tunnel zone; Wall, arena wall zone; mLength, mean length of time (seconds); range, range of distance traveled; entropy, entropy of movement in the x or y direction; kurtosis, kurtosis of the distribution of movement in the Y dimension; sdVelocity, standard deviation of velocity detected during the excursion; Total Gear Changes is the number of changes between slow, medium and fast velocity gaits; Mean Gear 2 Length is the mean length of bouts of medium velocity.